Indoor Climate Control Effect of AAC Panel Heat Capacity
Experimental rooms and simulations with three structural materials

YUKO TSUKIYAMA[1], NOBUYUKI SUNAGA[2], AKIKO SUZUKI[2], TAMAKI FUKAZAWA[2], YOSUKE CHIBA[1]

[1]Asahi Kasei Homes Corporation R&D Laboratories, 2-1 Samejima, Fuji-city, Shizuoka 416-8501 Japan
[2]Dept. of Architecture and Building Engineering, Tokyo Metropolitan University, 1-1 Minami-osawa, Hachioji, Tokyo 192-0397 Japan

ABSTRACT: The effect of autoclaved aerated concrete (AAC) heat capacity on indoor climate was investigated by experimental measurements and simulations with three mutually separated rooms having AAC, plywood (PW), or reinforced concrete (RC) floor and ceiling in a test house constructed for this purpose. Room temperature measurements showed the AAC room to be similar to the RC room in temperature trend during the day and to the PW room at night, and to keep temperature low as an effect of cooling storage even with short-term air conditioning. Floor surface measurements showed the daytime temperature rise to be largely limited to the area exposed to sunlight in the AAC and RC floor surfaces but extending throughout the PW floor surface. In the simulations, the AAC room cooling load with intermittent air conditioning was intermediate between those of the RC and PW rooms, and low room temperatures were more frequent in the AAC room than in the RC room. Some question remains, however, concerning the accuracy of temperature trend prediction in the AAC room, and further studies will be necessary to compare simulation predictions with experimental measurements and enhance their accuracy.
Keywords: AAC, heat capacity, thermal environment, experimental measurement, thermal load calculation

INTRODUCTION

The Kyoto Protocol and related trends have brought greater urgency to the task of reducing energy consumption in houses and thus reducing carbon dioxide emissions. In residences, in particular, effective passive design for utilization of environmental energy for this purpose is particularly important and challenging, as indoor thermal comfort is prerequisite.

Studies on passive design have generally focused on reinforced concrete and brick structures, which are high in heat capacity, and wooden structures, which are low in heat capacity [e.g., 1]. Little has been reported, however, on structures with intermediate heat capacity, such as autoclaved aerated concrete (AAC).

AAC panels, whose thermal conductivity of 0.17 W/mK and volumetric heat capacity of 600 kJ/m^{3}K are similar to those of plywood, are generally used in thicknesses of 50~100 mm in Japan. Their heat capacity may thus be expected to significantly affect indoor climate.

In the present study, we therefore constructed an experimental house (Fig. 1, 2) containing mutually separated rooms with AAC, plywood (PW), or reinforced concrete (RC) floor and ceiling, and investigated their

Figure 1: Experimental house viewed from southwest.

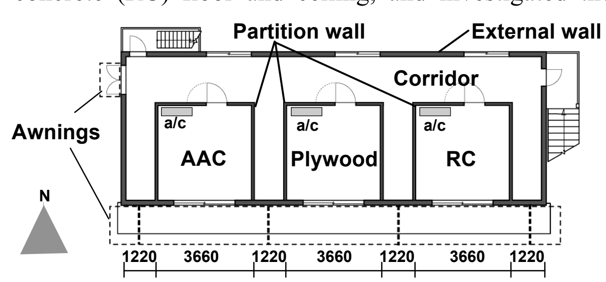

Figure 2: Experimental house floor plan (second-story level).

respective thermal effects by experiment and simulation.

EXPERIMENTAL METHODOLOGY

Experimental house and room structure The experimental house was constructed at Fuji City, Shizuoka Prefecture in August 2008, with the test rooms raised to the second-floor level on square steel pillars (Fig. 1) to avoid sun and wind blockage, and the floor plan (Fig. 2) designed for direct sunlight exposure only on the south wall of the rooms and for separation of the rooms from each other and from the north, east, and west external wall by corridor and buffer spaces. The external wall on all four sides was constructed with AAC, the floor and ceiling in each room with AAC, plywood (PW), or RC, and the partition wall on three sides of each room with plasterboard, as shown in Table 1 together with their thermal transmittances. The components were selected to provide equivalent thermal transmittance for all the three rooms and to meet the Next-generation Energy-saving Standard in Japan (Area IV). Each room had a floor space of 13.4 m^2 and ceiling height of 2.665 m, one opening in its south wall measuring 2.279 x 1.980 m and consisting of double-glazed low-e glass with aluminium-plastic composite sash frames, and removable awnings projecting 1.5 m horizontally and vertically from the wall to shield against direct exposure to sunlight in summer.

Calculation of effective heat capacity In the present study, we applied two of the various methods for the calculation of the heat capacity which effectively acts to influence room temperature, termed "effective heat capacity" [2]: Method 1, which well expresses the characteristics of room temperature variation in RC structures, and is based on analytical solution of the variation in the internal temperature of the wall material [2]; and Method 2, which is relatively simple and widely employed, and is based on the heat capacity of the effective thickness of the material inside the insulation [3]. As shown in Table 2, the values obtained by Methods 1 and 2 were nearly equal for the AAC room, but were in the ratio of approximately 1.2 for the PW room and the reverse ratio for the RC room. These differences are directly attributable to their differing ceiling and floor materials, as all three rooms were entirely the same in the composition of their partition walls and south external wall. The ratio of the values obtained for the AAC, PW, and RC rooms was 1:2:9 by Method 1, and 1:2.5:14 by Method 2, which yielded a particularly high value for the RC room.

Measurement conditions and modes All measurements were made in September 2008, using T-type thermocouples, globe thermometers, pyrano-meters, and hotwire anemometers positioned as shown in Fig. 3 and 4. The surface temperature was measured at 600 mm intervals over the southern half of each floor. Two

Table 1: Room structures (SB: calcium silicate board, PF: phenolic foam, PB: plasterboard, RW: rock wool, Next-generation Energy-saving Standard (Area IV) values shown in parentheses.

	PW room	AAC room	RC room
Ceiling	Plywood 12 air Plywood 12 PF85 Plywood12	CSB 6 PF70 AAC100	CSB 6 PF80 RC150
(0.24W/m^{2}K)	U=0.232W/m^{2}K	U=0.235W/m^{2}K	U=0.235W/m^{2}K
Floor	Plywood 12 PF55 Plywood 12	AAC100 PF40	RC150 PF50
(0.34W/m^{2}K)	U=0.338W/m^{2}K	U=0.347W/m^{2}K	U=0.346W/m^{2}K
Wall	External Wall (inside) AAC 75 air PF 25 air PB 125	Partition Wall PB 125 air RW 55 air PB 125	
	U=0.488W/m^{2}K(0.53W/m^{2}K)	U=0.489W/m^{2}K	
Window	Double-glazed Low-e glass	U=2.91W/m^{2}K	

Table 2: Effective heat capacities, by Methods 1 and 2.

	Effective Heat Capacity Method 1 DKJ/KE			Effective Heat Capacity Method 2 DKJ/KE		
	PW	AAC	RC	PW	AAC	RC
Ceiling	167.6	547.0	3042.0	112.8	529.9	3885.7
Floor	144.4	534.1	3029.1	112.8	529.9	3885.7
South external wall	80.0	80.0	80.0	56.1	56.1	56.1
Partition wall	319.6	319.6	319.6	294.8	294.8	294.8
Sum total	711.6	1480.7	6470.7	576.5	1410.6	8122.2

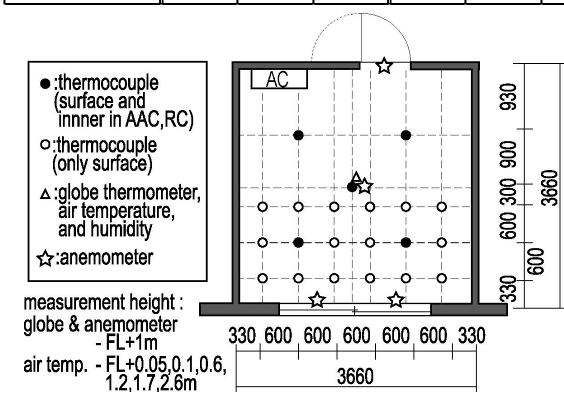

Figure 3: Measurement points in each room.

Figure 4: Interior views of RC room.

Table 3: Experimental modes.

	Mode	Window open	Air conditioning("a/c")	Day
1	Cross ventilation	All day		9/5; 8
2	Cross ventilation at night	18:00; 9:00		9/24; 27
3	Intermittent a/c 26°C		7:00; 9:00,18:00; 24:00	9/9; 12
4	Intermittent a/c 20°C		7:00; 9:00,18:00; 24:00	9/13; 19
5	Continuous a/c 20°C		All day	9/20; 23

incandescent light bulbs were left on in each room from 7:00 to 9:00 and 18:00 to 24:00, to simulate human body warmth emission.

As shown in Table 3, the five experimental modes were: Mode 1 with round-the-clock cross ventilation; Mode 2 with cross ventilation at night only; Mode 3 with intermittent air conditioning (a/c) set to 26˚C; Mode 4 with intermittent a/c set to 20˚C; and Mode 5 with continuous a/c set to 26˚C. The room condition was reset between modes by leaving the window open from 9:30 to 17:30.

EXPERIMENTAL RESULTS

Cross-ventilation modes Fig. 5 (Mode 1) and Fig. 6 (Mode 2) show the air temperature 1.2 m above the floor in the middle of the room (hereinafter the “room temperature”) and the floor surface temperature in the same part of the room (hereinafter the “central floor surface temperature”). Fig. 7 shows the relation between outdoor air temperature and the area-weighted average temperature of the floor surface for each room in Modes 1 and 2 on representative days.

In Mode 1, the room temperatures were generally the same in all three rooms and matched the outdoor temperatures except for a slight elevation at night due to heating by the light bulbs. The central floor surface temperatures closely followed the room temperatures in the AAC room throughout, but were higher than the room temperatures during the day in the PW room and at night in the RC room.

In Mode 2, the night-time room temperatures in all three rooms again generally matched the outdoor temperatures. The daytime room temperatures, in contrast, showed differing patterns. In the PW room, they were well above the outdoor temperatures despite the shading provided by the 1.5 m awning above the window of each room in the south wall. In the AAC room, though much lower than in the PW room, they were above the outdoor temperatures, particularly as the latter began to fall at 15:00 and for several hours thereafter. In the RC room, they were at or below the outdoor temperature until about 15:00, due to the night-time cooling storage of the RC, but above the outdoor temperatures by 16:00 and thereafter, though less so than the AAC room. The Mode 2 floor temperature in the AAC room was generally intermediate between those of the PW and RC rooms, but with minimum values similar to those of the PW room. In comparison with the AAC room temperature, it was characterized by a more moderate daytime rise from about the same night-time minimum.

Air conditioned modes Fig. 8 shows the room temperatures and central floor temperatures in Mode 4. In all three rooms, the room temperature was near the a/c setting of 20˚C while the a/c was on during the a/c

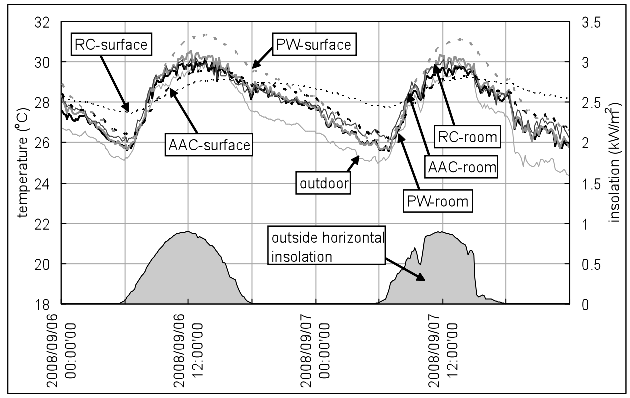

Figure 5: Temperature and insolation patterns, Mode 1.

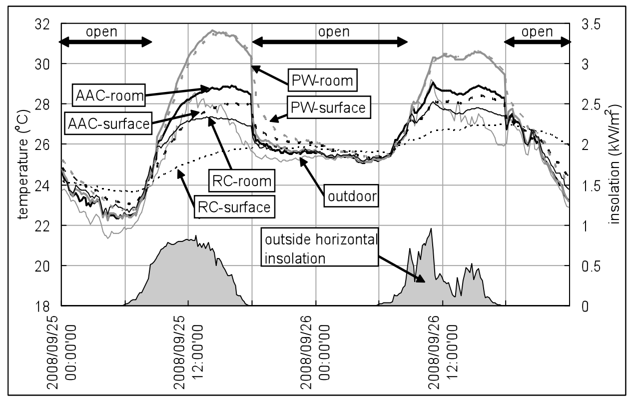

Figure 6: Temperature and insolation pattern, Mode 2.

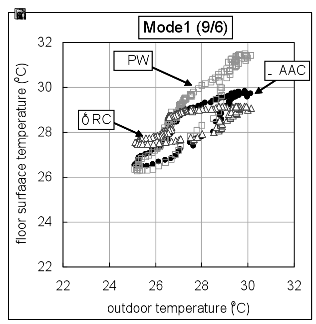

Figure 7: Central floor surface and outdoor temperatures, Modes 1 & 2.

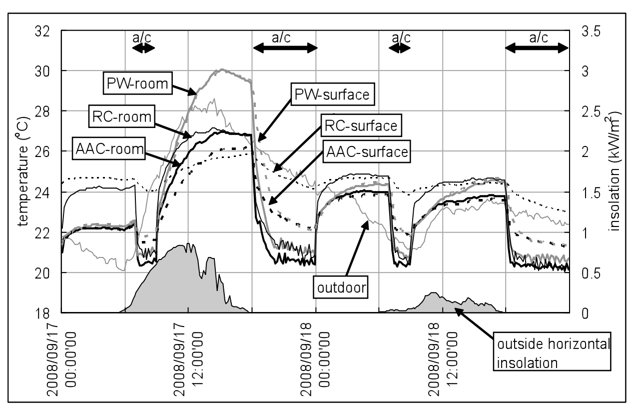

Figure 8: Temperature and insolation patterns, Mode 4.

periods of 7:00 to 9:00 and 18:00 to 24:00. After the a/c was turned off at 9:00, the PW room temperature on September 17th rose sharply for the sunlight exposure and peaked 3˚C above the outdoor temperature, but the AAC and RC room temperatures rose more moderately and remained below the outdoor temperature until late afternoon, as an effect of their greater cooling storage during the morning a/c period. The cooling storage effect of AAC is clearly shown by the approach of the AAC room temperature pattern to that of the RC room in Mode 4 during the day, in contrast to the difference between the patterns of the two rooms during night-time ventilation in Modes 1 and 2. The Mode 4 central floor surface temperature also showed the differing effects of the three materials. In the PW room, it was practically the same as the room temperature night and day, but in both the AAC and the RC rooms it remained below the room temperature throughout the day. In the RC room at night, however, it remained comparatively high. During the 6-hour a/c period, it declined only 2˚C while the room temperature declined about 6˚C. In the AAC room, the daytime central floor surface temperature rise was similar to that of the RC room and the night-time decline similar to that of the PW room; the daytime rise was thus more moderate than in both of the other rooms.

The results suggest that, although the a/c periods were rather short for RC cooling, they were sufficient for cooling storage of AAC, as an effect of its lower effective heat capacity. Fig. 9 shows the daily cooling loads, room temperatures, and outdoor temperatures in Modes 3 to 5. Cooling load was calculated from the temperature and flow rate of water leaving the outdoor unit, and returning to it from the indoor unit, in the circulating water a/c system for each room. Under intermittent a/c, the cooling load generally increased with the effective heat capacity of the floor and ceiling material, and the difference between the three rooms in cooling load was clearly larger at the 20˚C setting than at the 26˚C setting. Although the AAC room required a lower cooling load than the RC room, its maximum and average room temperatures were nearly the same in the RC room, thus suggesting that AAC can provide a comfortable indoor temperature with a comparatively low cooling load. Under continuous a/c, the difference between the three rooms in cooling load was larger on the first day than on the second day, on which the AAC room cooling loads was nearly the same as that of the RC room. It is probable that the difference between the cooling loads would have become negligible on subsequent days in accordance with the widely recognized tendency for differences between cooling loads to decrease with time under extended continuous a/c with equivalent insulation.

Floor surface temperature patterns in Mode 1 Fig. 10 shows the surface temperature patterns on the floor of each room in Mode 1 (24-hour cross-ventilation) at 3-

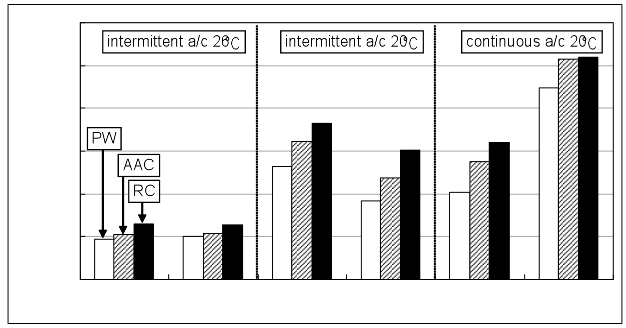

		9/10	9/11	9/17	9/18	9/22	9/23
outdoor	max.	28.3	29.5	28.6	24.3	23.5	26.8
temp.	ave.	24.4	24.4	24.5	22.8	22.2	23.7
(°C)	min.	20.3	19.1	20.1	21.2	21.1	20.5
insolation (kJ/day)		23480	20927	19607	4388	4580	18672

Figure 9: Cooling load and room and outdoor temperatures.

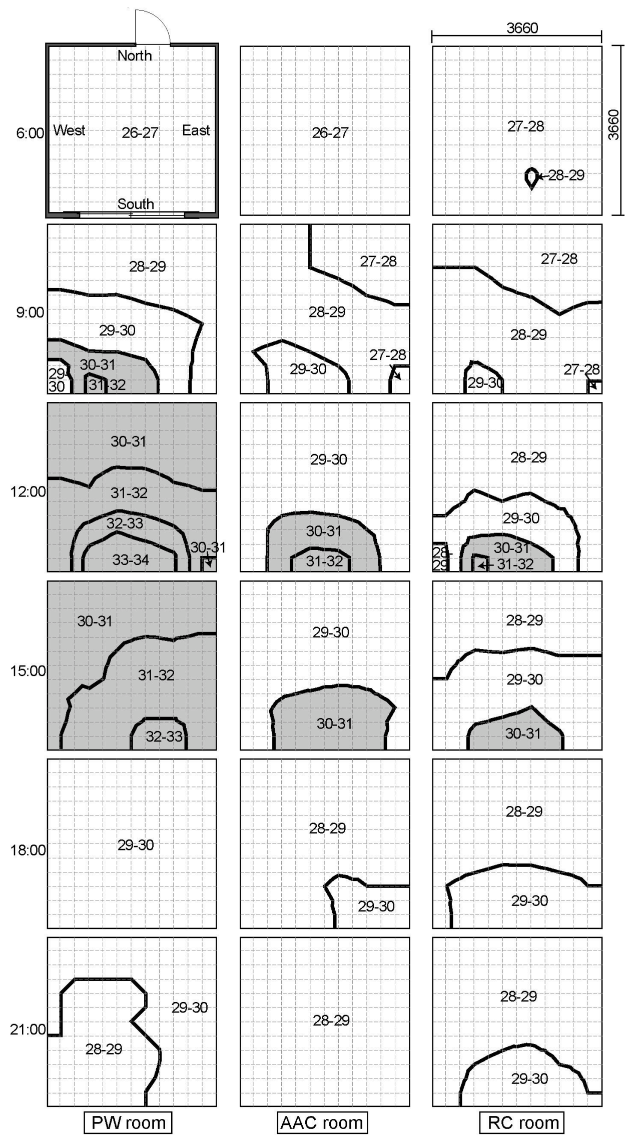

Figure 10: Floor surface temperatures (in ˚C), Mode 1.

hour intervals (9:00 to 21:00) on September 6. Although the three rooms showed almost no difference in room temperature (Fig. 5), the PW floor underwent large fluctuations in surface temperature, with a comparatively large rise throughout its surface as well as in the southern portion under southern sunlight exposure and decline between 18:00 and 21:00 under air flow from the window in the south wall. The temperature rise on the AAC floor was smaller and much more localized to the southern portion than on the PW floor. In the RC room, the temperature elevation was even smaller and more localized than on the AAC floor during the day, but clearly more persistent in the hours after 18:00 due to its greater heating storage during the day.

SIMULATION METHODOLOGY

The simulations were performed for a far longer term (3 months) and many more modes (11) than was possible in the experiments, using the TRNSYS multi-zone dynamic thermal simulation program [6] and the COMIS multi-zone ventilation volume simulation program [7], as indicated in Table 4, to calculate indoor temperatures and cooling loads. The room models and all structural layers were the same as in the experiments, but they were located on the first-floor level with the under floor space. Wether data was taken from the Expanded AMeDAS weather data for Yoshiwara City, Shizuoka Prefecture [8] where is near the construction area of the experimental house. As in the experiments, room heating at 200 W was applied from 7:00 to 9:00 and 18:00 to 24:00.

The eleven simulated modes (distinguished from the experimental modes by suffix "s") are shown in Table 5. All modes except Mode 1s included the awnings. Modes 1s to 5s were without a/c: Mode 1s and 2s window closed, Mode 3s with window open throughout, and Modes 4s and 5s with window open 9:00 to 18:00 and 18:00 to 9:00 respectively. Modes 6s to 11s were with continuous or intermittent a/c set to 26˚C or 20˚C and window closed throughout or open 0:00 to 7:00.

SIMULATION RESULTS

Indoor temperature The results of the simulation for Modes 5s and 7s on the typical summer days of August 5 and 6 provide a basis for assessment of the simulation methodology and results by comparison with the results of the Mode 2 and Mode 4 experiments under the same respective conditions.

The temperature patterns obtained in Mode 5s (Fig. 11) closely matched with those in Mode 2 (Fig. 6). For the PW and RC rooms, the two modes gave almost exactly the same results. For the AAC room, the room and central floor surface temperatures were somewhat higher in Mode 5s than in Mode 2, but followed essentially the same pattern in both two modes.

Table 4: Simulation base.

Simulation program	TRNSYS 16_1, COMIS	
Meteological date	Expanded AMeDAS weather date	
	Area$Yoshiwara, Shizuoka, Standard year	
Calculation period	7/1; 9/30 D approach 2weeks:6/17; E	
Internal heat gain	720kJ/h D7:00; 9:00 18:00; 24:00E	

Table 5: Simulation modes.

Mode	Awnings	Window schedule		Air conditioning(a/c)	
		Open/Close	Time	On/Off	Time
1s	×	Close		Off	
2s	o	Close		Off	
3s	o	Open	All day	Off	
4s	o	Open	9:00; 18:00	Off	
5s	o	Open	18:00; 9:00	Off	
6s	o	Close		On26°C	7:00; 9:00,18:00; 24:00
7s	o	Close		On20°C	7:00; 9:00,18:00; 24:00
8s	o	Close		On26°C	All day
9s	o	Close		On20°C	All day
10s	o	Open	24:00; 7:00	On26°C	7:00; 9:00,18:00; 24:00
11s	o	Open	24:00; 7:00	On20°C	7:00; 9:00,18:00; 24:00

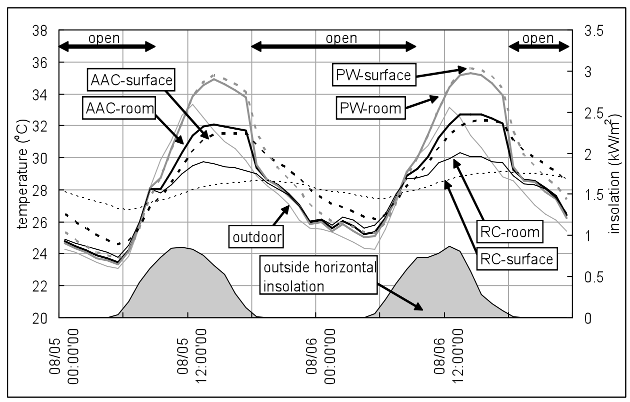

Figure 11: Temperature and insolation patterns, Mode 5s.

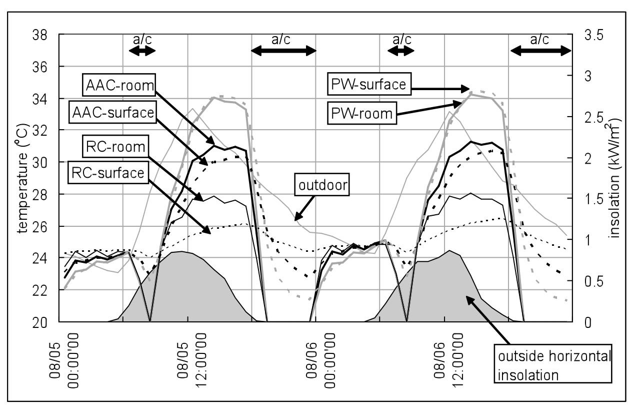

Figure 12: Temperature and insolation patterns, Mode 7s.

Some disagreement was observed, however, between the results in Modes 7s and 4 (both with intermittent a/c set to 20˚C). In Mode 4, the room temperatures of the AAC and RC rooms were nearly the same throughout. In Mode 7s, in contrast, the AAC room temperatures were generally intermediate between those of the other two rooms. A similar disagreement was observed between the

	Cooling Load (MJ/Month)		
	PW	AAC	RC
6s	350.2	408.7	461.2
7s	767.4	875.1	994.0
8s	710.1	709.2	707.8
9s	1615.1	1632.0	1633.7
10s	333.7	375.0	380.9
11s	758.4	869.6	994.6

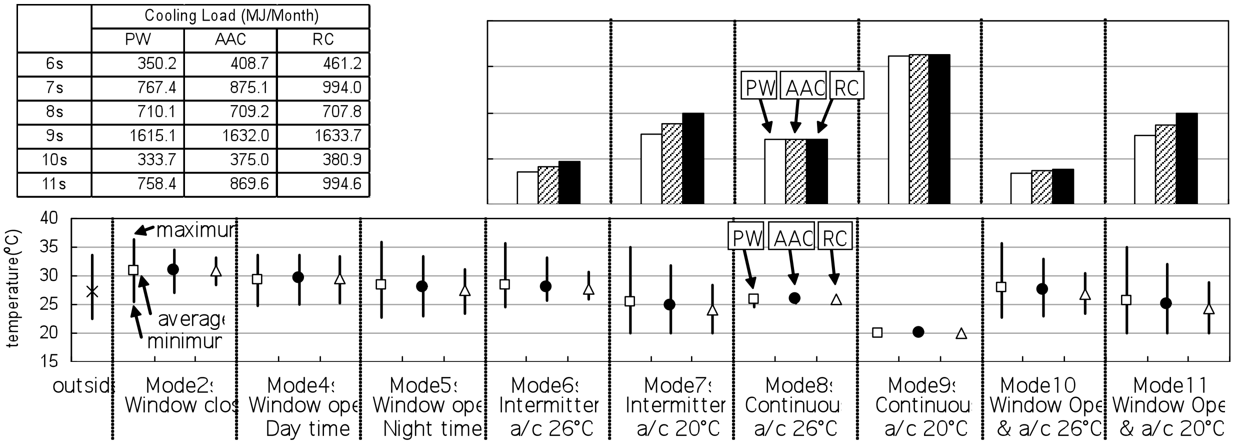

Figure 13: Cooling loads and room and outdoor temperature ranges in August.

experimental and simulation results with an intermittent a/c setting of 26˚C. It is not certain whether this disagreement was caused by the simulation methodology or by a residual effect from the previous weeks in the simulation, and further study is planned to resolve this question, in the awareness that an error may have occurred in the AAC room simulation.

Cooling load Fig. 13 shows the room temperature ranges and cooling loads in August. The room temperature range narrowed in the order RC, AAC, and PW in the non-a/c modes with the window closed throughout or open at night (2s and 5s) and in all intermittent a/c modes (6s, 7s, 10s, and 11s), and the cooling load in all intermittent a/c modes narrowed in the order PW, AAC, and RC. This may be attributable to the intermediate and high effective heat capacities of AAC and RC. In Mode 10s, with intermittent a/c set to 26˚C and the window open from 0:00 to 7:00, the differences in cooling load became quite small, suggesting that night-time cross-ventilation might be effectively employed to reduce the cooling load with materials having high effective heat capacity. In the two modes with continuous a/c (8s and 9s), the cooling load was essentially the same for all three rooms due to their equivalent thermal transmittances.

Temperature frequency distribution during a/c shutoff Fig. 14 shows the room temperature frequency distributions in the three rooms during the periods (0:00 to 7:00 and 9:00 to 18:00) when the intermittent a/c set to 26˚C was not operating. As shown, the distribution tended to widen and the maximum temperature tended to increase with decreasing effective heat capacity. The RC room temperature did not rise above 31˚C at any time during the month and was thus the lowest maximum among the three rooms. It showed a tendency to stay rather high and never fell to 26˚C or lower, again suggesting that the intermittent a/c modes in this study were insufficient for fully effective RC cooling. The AAC room temperature was most frequently in the vicinity of the 26˚C a/c setting, but it also rose above

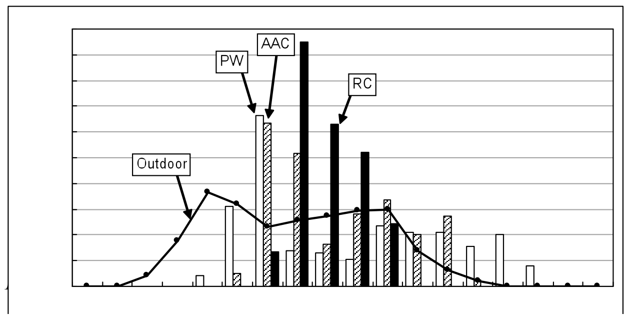

30˚C rather frequently, suggesting that combination with cross-ventilation is desirable to maintain low room temperatures without increasing the cooling load.

CONCLUSION

The summer measurements in the experimental house showed the AAC thermal characteristics to include moderation of daytime temperature rise, rather rapid evening temperature decline, and rather rapid cooling storage and release. In the simulations, AAC showed room temperatures somewhat higher than in the experimental measurements, room cooling loads under intermittent a/c intermediate between those with either PW and or RC, and a greater low temperature frequency than with RC. Further study will be necessary, for comparison of longer-term experimental results with those of the present short-term experiments and confirmation on the accuracy of the present simulation.

REFERENCES

1. F. Hasegawa. et al (1986), Experimental Study on Thermal Storage Floor System of Passive Solar Systems Using an Actual Test House. *Journal of Architecture*, 366: p.33-41
2. N. Sunaga (1992), Study on The Effect of Thermal Mass on Indoor Climate Control with Solar Energy: p.171-174.
3. Design Guideline to Independent Cycle House (2005), Institute for Building Environment and Energy Conservation.
4. TRNSYS 16 (2007), A Transient System Simulation Program, User Manuals: Solar Energy Laboratory, University of Wisconsin-Madison.
5. COMIS 3.2 (2005), Conjunction of Multizone Infiltration Specialists, EMPA.
6. Expanded AMeDAS Weather Data (2005), Architectural Institute of Japan.